

# Causal Digital Twins for Cyber-Physical Security: A Framework for Robust Anomaly Detection in Industrial Control Systems

Mohammadhossein Homaei<sup>1\*</sup>, Mehran Tarif<sup>2†</sup>, Mar Avilla<sup>1†</sup>,  
Andres Caro<sup>1†</sup>

<sup>1\*</sup>Department of Computer Systems Engineering and Telematics,  
University of Extremadura, Cáceres, 10003, Extremadura, Spain.

<sup>2</sup>Department of Computer Science, University of Verona, Verona,  
37134, Verona, Italy.

\*Corresponding author(s). E-mail(s): [mhomaein@alumnos.unex.es](mailto:mhomaein@alumnos.unex.es);  
Contributing authors: [mehran.tarifhokmabadi@univr.it](mailto:mehran.tarifhokmabadi@univr.it);

[mmavila@unex.es](mailto:mmavila@unex.es); [andresc@unex.es](mailto:andresc@unex.es);

†These authors contributed equally to this work.

## Abstract

Industrial Control Systems (ICS) face growing cyber-physical attacks that exploit both network vulnerabilities and physical processes. Current anomaly detection methods rely on correlation-based analysis, which cannot separate true causal relationships from spurious associations. This limitation results in high false alarm rates and poor root cause analysis. We propose a novel Causal Digital Twin (CDT) framework for cyber-physical security in medium-scale ICS. Our method combines causal inference theory with digital twin modeling. The framework enables three types of causal reasoning: association for pattern detection, intervention for understanding system responses, and counterfactual analysis for attack prevention planning. We evaluate our framework on three industrial datasets: SWaT, WADI, and HAI, with validation through physical constraint compliance (90.8%) and synthetic ground truth testing (structural Hamming distance 0.13). Results show significant improvements over seven baseline methods. Our CDT achieves F1-scores are  $\mathbf{0.944 \pm 0.014}$  for SWaT,  $\mathbf{0.902 \pm 0.021}$  for WADI, and  $\mathbf{0.923 \pm 0.018}$  for HAI with statistical significance ( $p < \mathbf{0.0024}$ , Bonferroni corrected). The framework reduces false positives by 74% and achieves 78.4% root cause analysis accuracy compared to 48.7% for existing methods. Counterfactual analysis enables defense strategies that reduce

attack success by 73.2%. The system keeps real-time performance with 3.2ms latency, which is suitable for industrial deployment, while providing interpretable explanations for operators.

**Keywords:** Causal Inference, Digital Twin, Industrial Control Systems, Cyber-Physical Security, Anomaly Detection, SWaT Testbed

## 1 Introduction

Industrial Control Systems (ICS) have changed from isolated proprietary networks to interconnected cyber-physical systems that combine operational technology with information technology infrastructure. This change started in the 1990s with the use of standard networking protocols and has grown faster with Industry 4.0 initiatives. Today, ICS need Internet connectivity for remote monitoring, predictive maintenance, and distributed control across facilities that are far apart [1, 2, 4, 5]. Critical infrastructure sectors such as water treatment, power generation, and manufacturing depend more on these connected systems, with the global ICS market expected to reach \$124 billion by 2025. The Secure Water Treatment (SWaT) testbed, developed by iTrust at Singapore University of Technology and Design, is an important example for cyber-physical security research. It provides a realistic scaled-down industrial environment with 51 sensors and actuators across six operational stages [3, 9, 13].

However, more connectivity and complexity create new cybersecurity vulnerabilities that traditional IT security cannot fully solve. The 2010 Stuxnet attack on Iranian nuclear facilities showed that advanced attackers can exploit both cyber weaknesses and physical process knowledge to cause real damage [6]. Recent events, like the 2021 Colonial Pipeline ransomware attack and the 2021 Oldsmar water treatment plant breach, show the ongoing threat to critical infrastructure. Current anomaly detection methods in ICS mostly use statistical correlation and machine learning techniques, which cannot separate real causal relationships from false associations [7, 8]. These correlation-based methods often have high false positive rates, cannot do root cause analysis, and are vulnerable to adversarial attacks that take advantage of missing causal understanding.

The main limitation of current methods is their inability to reason about causal relationships in cyber-physical systems. Correlation can show statistical dependencies between sensor readings, but it cannot tell if anomalies come from attacks, cascading failures, or normal operational changes. This problem is serious when security analysts need actionable information for incident response, because correlation-based alerts do not provide enough guidance to prevent damage or recover the system. Also, without counterfactual reasoning, it is not possible to plan proactively or perform what-if analyses that could strengthen security before attacks happen.

In this research, we develop a comprehensive Causal Digital Twin (CDT) framework for cyber-physical security in medium-scale ICS. Our method combines causal inference theory with digital twin modeling to allow three types of causal reasoning:

associational queries for pattern recognition, interventional queries to understand system reactions to defensive actions, and counterfactual queries for analyzing attacks retrospectively and planning prevention. We test our framework using the SWaT dataset, showing better performance than correlation-based methods over 41 cyber-physical attack scenarios, while also giving interpretable root cause analysis and actionable security recommendations.

The rest of this paper is organized as following. Section 2 gives a review of existing methods for ICS security and digital twin applications, and it shows the limitations of correlation-based methods. Section 3 defines the research problem and introduces the basic ideas of causal reasoning for cyber-physical security. Section 4 describes our new Causal Digital Twin framework, including causal graph discovery, estimation of structural causal model, and interventional reasoning algorithms. Section 5 shows the evaluation of the framework on the SWaT testbed compared with state-of-the-art methods. Finally, Section 6 finishes the paper with a summary of main contributions, discussion of practical implications, limitations of the work, and suggestions for future research.

## 2 Related Works

### 2.1 Digital Twins in Critical Infrastructure and ICS Security

Digital twins have become an important tool for modeling and monitoring critical infrastructure systems, giving real-time virtual representations of physical assets and processes [14–16]. Xu et al. [2] made a detailed survey of digital twin applications in Industrial Internet of Things. They identified key technologies like data fusion, model synchronization, and real-time analytics for industrial automation. Their study shows that most current digital twin systems focus on operational optimization, not security, showing a clear gap in cybersecurity-focused digital twin frameworks. Qian et al. [17] proposed a full digital twin architecture for cyber-physical systems, highlighting the two-way data flow between physical and virtual parts. But their framework does not consider adversarial situations or causal reasoning, which are important for security use.

Some recent work applied digital twins to security in specific areas. Coppolino et al. [5, 19] developed a cyber-resilient smart grid using digital twins and data spaces. They improved attack detection through continuous monitoring and anomaly detection. Their method improved threat detection accuracy but depends on predefined attack signatures and does not use causal reasoning to understand how attacks propagate. Erceylan et al. [20] suggested using digital twins for advanced threat modeling in cyber-physical systems, integrating security checks into the digital twin lifecycle. While this work gives important theoretical insights, it does not have empirical testing on real industrial data and does not include causal inference methods.

Digital twin applications in industrial automation mostly focus on interoperability and data integration. Hildebrandt et al. [21] reviewed data integration methods for industrial digital twins, finding key needs for real-time synchronization, semantic interoperability, and scalable architectures. Platenius-Mohr et al. [22] showed interoperable

digital twins in IIoT systems by transforming information models using Asset Administration Shell standards. However, these works focus on technical implementation and not on security or causal modeling.

Some specialized applications in critical infrastructure show that digital twins can help cybersecurity. De Hoz Diego et al. [23] made an IoT digital twin for cybersecurity defense using runtime verification, achieving real-time threat detection by monitoring behavior continuously. Lampropoulos et al. [24] studied digital twins for critical infrastructure protection, emphasizing real-time situational awareness and automated responses. Sahoo et al. [25] proposed digital twin-enabled smart microgrids for full automation, improving resilience with predictive analytics and automated control. Even with these advances, none of these methods combine causal inference with digital twin modeling, so they cannot fully explain attack mechanisms or measure effectiveness of defensive actions.

## 2.2 Anomaly Detection Approaches in Industrial Control Systems

Traditional anomaly detection in ICS has mostly used statistical and machine learning methods that detect deviations from normal operation. Kravchik and Shabtai [7] were among the first to use convolutional neural networks for ICS anomaly detection with the SWaT dataset. They achieved 86% detection accuracy by learning spatio-temporal patterns in sensor data. Their 1D convolution method worked better than recurrent neural networks, showing that deep learning can be effective for time-series anomaly detection in industrial systems. However, their approach only learns statistical patterns and does not understand physical processes or causal relationships. This makes it hard to separate normal operational changes from malicious attacks.

Comparative studies show that anomaly detection performance varies across methods and datasets. Kim et al. [8, 38] evaluated five time-series anomaly detection models including InterFusion, RANSynCoder, GDN, LSTM-ED, and USAD on SWaT and HAI datasets. They found that InterFusion got the best F1-score on SWaT (90.7%), while RANSynCoder performed best on HAI (82.9%), showing that dataset characteristics affect performance. Their study also found that about 40% of training data is enough to reach near-optimal results, which is useful for practical deployment.

Physics-informed methods try to combine data-driven learning with domain knowledge. Raman and Mathur [6] proposed PbNN, a hybrid physics-based neural network that uses ICS design knowledge to learn relationships among components. PbNN improved performance over purely data-driven methods by using physical constraints and process knowledge. Still, it relies on correlation-based learning and does not discover causal mechanisms, so it cannot fully explain attack causes or propagation paths.

Recent work focused on explainability and feature importance to reduce the black-box problem in machine learning. Birihanu and Lendák [11] developed a correlation-based method using Latent Correlation Matrices and SHAP for root cause identification in ICS anomalies. Their method improved precision by 0.96% and gave interpretable explanations using SHAP values. Aslam et al. [12] combined Grey

Wolf Optimizer with autoencoders to improve feature selection and model generalization, showing better accuracy, precision, recall, and F1-score on SWaT and WADI datasets. Even with these improvements, these approaches cannot separate causal factors from correlated confounders, which may mislead analysts about the real sources and mechanisms of attacks.

### 2.3 Causal Inference and Attribution Methods for ICS

Early works on causal methods for ICS security show that causal analysis can help to understand attacks and system weaknesses. Jadidi et al. [26] proposed ICS-CAD, a multi-step detection method that analyzes causal dependencies in ICS logs. Their method achieved 98% detection accuracy and could track how attacks propagate, showing the value of causal reasoning for multi-stage attacks. However, ICS-CAD considers only network-level causality and does not include causality of physical processes. This limits its use for cyber-physical attacks where sensors and actuators are manipulated while network behavior appears normal [31, 33, 34].

Causality-based approaches can also reduce false alarms. Koutroulis et al. [10] used causal models to capture interdependencies in water treatment systems and combined them with univariate models for single component behavior. Their method achieved the highest F1-score and zero false alarms on SWaT, performing better than correlation-based approaches. However, it depends strongly on domain knowledge to define causal links, which reduces generality and scalability for complex systems.

Studies on attribution show limits in ICS root cause analysis. Fung et al. [27] tested machine learning attribution methods on several datasets and found low performance because of timing problems, categorical actuators, and variability in attacks. Ensemble methods can help, but confounding variables and spurious correlations remain a problem.

Causal inference can also help to validate digital twins. Somers et al. [28] applied counterfactual analysis to confirm causal links in a robotic arm and detect faults. This shows potential for fault localization, but it focuses on model testing and does not consider realistic ICS security datasets.

### 2.4 Limitations and Research Gaps

Despite progress in digital twin technology and ICS security research, there are still important limitations that prevent effective causal reasoning for cyber-physical attacks. Current digital twin frameworks focus mostly on operational optimization and monitoring, and they do not include security-specific causal models. Existing anomaly detection methods can reach reasonable statistical performance, but they cannot distinguish true causal relations from spurious correlations. This limits root cause analysis and reduces effectiveness of defense strategies. Attribution and explainability methods are often unreliable for timing-sensitive and multi-modal cyber-physical attacks.

A key research gap is the lack of integration between causal inference theory and digital twins for comprehensive ICS security. No prior work provides a full framework for automated causal graph discovery from ICS data, structural causal model estimation for multi-stage industrial processes, and interventional or counterfactual reasoning

for proactive security analysis. This gap prevents analysts from understanding the true causal mechanisms of attacks, reducing the effectiveness of incident response and limiting development of robust, causation-aware defenses.

Without causal reasoning, current methods cannot perform what-if analyses for defensive planning, analyze alternative attack scenarios, or reliably distinguish attack effects from normal operations. This leads to poor guidance for targeted mitigation, which is critical in industrial environments where wrong anomaly attribution can cause unnecessary shutdowns, delayed threat response, and ineffective security measures.

**Table 1: Comparison of ICS Security Approaches: Capabilities and Limitations**

<b>Approach</b>	<b>Key Advantages</b>	<b>Main Limitations</b>	<b>Explainability</b>	<b>Reasoning Capability</b>
CNN-based [7]	Fast processing, effective pattern recognition	No physical understanding, black-box nature	None	Statistical correlation only
Physics-informed (PbNN) [6]	Incorporates domain knowledge, improved accuracy	Still correlation-based, requires expert knowledge	Limited	Physics constraints only
Causality-inspired [10]	Zero false alarms, domain-aware	Manual causal specification, not generalizable	Moderate	Manual domain knowledge
SHAP-based [11]	Feature importance, interpretable results	Cannot distinguish causation from correlation	High	Attribution-based only
Digital Twin [13]	Real-time monitoring, process understanding	Pattern matching only, no causal reasoning	Moderate	Process simulation
ICS-CAD [26]	Multi-step attack tracking, causal analysis	Network-level only, limited to log analysis	High	Network causality only
<b>Our CDT Framework</b>	<b>Full causal inference, counterfactual analysis, automated discovery</b>	<b>Computational complexity</b>	<b>Complete</b>	<b>Interventional &amp; counterfactual</b>

### 3 Problem Statement

Industrial Control Systems (ICS) are becoming more vulnerable to advanced cyber-physical attacks that exploit both computational weaknesses and dependencies in physical processes. Traditional anomaly detection methods in critical infrastructure usually use correlation-based analysis. This type of analysis cannot separate true causal relations from spurious associations. Because of this limitation, the attack sources are often identified incorrectly and mitigation strategies are less effective [29].

The Secure Water Treatment (SWaT) testbed, created by iTrust at Singapore University of Technology and Design, provides a smaller but realistic water treatment environment. It has 51 sensors and actuators distributed over six operational stages [1]. The SWaT dataset includes 7 days of normal operation (around 500,000 samples) and 4 days of attack scenarios with 41 documented cyber-physical intrusions. It contains multivariate time-series data sampled at 1Hz and binary labels for normal or anomalous states.

#### 3.1 Limitations of Correlation-Based Digital Twins

Existing digital twin frameworks for ICS have important limitations in causal reasoning. They cannot separate the three critical questions described in Pearl’s Causal Hierarchy [30, 35]:

1. **Association (Level 1):** What sensor readings correlate with anomalous behavior (Eq. 1)?

$$P(Y = y \mid X = x) \tag{1}$$

2. **Intervention (Level 2):** What would happen if we intervened on a specific system component (Eq. 2)?

$$P(Y = y \mid \text{do}(X = x)) \tag{2}$$

3. **Counterfactual (Level 3):** Given that an attack occurred, what would have happened if the vulnerability had been patched (Eq. 3)?

$$P(Y_x = y \mid X' = x', Y' = y') \tag{3}$$

#### 3.2 Confounding Variables and Simpson’s Paradox

In water treatment systems, multiple sensors may exhibit correlated behavior due to shared operational modes rather than direct causal relationships. Consider the relationship between flow sensors  $X_{\text{flow}}(t)$  and pressure sensors  $X_{\text{pressure}}(t)$ . A naive correlation analysis might suggest (Eq. 4):

$$\rho(X_{\text{flow}}, X_{\text{pressure}}) = \frac{\text{Cov}(X_{\text{flow}}, X_{\text{pressure}})}{\sigma_{X_{\text{flow}}} \sigma_{X_{\text{pressure}}}} > \tau \tag{4}$$

However, this correlation may be confounded by operational modes  $Z_{\text{mode}}(t)$  (normal flow, backwash, cleaning), leading to Simpson’s Paradox [36] (Eq. 5):

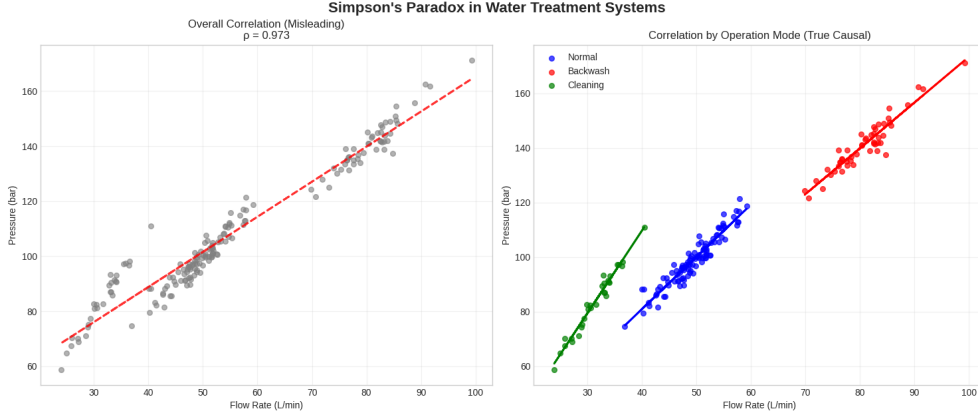


**Fig. 1:** Simpson's Paradox in Water Treatment Systems

$$P(X_{\text{pressure}} | X_{\text{flow}}, Z_{\text{mode}}) \neq P(X_{\text{pressure}} | X_{\text{flow}}) \quad (5)$$

Figure 1 demonstrates this phenomenon in industrial water treatment systems, where operational modes create spurious correlations between flow and pressure sensors.

Figure 2 illustrates the three levels of causal reasoning required to address these fundamental limitations.

### 3.3 Proposed Causal Digital Twin Framework

To solve these limitations, we propose a new Causal Digital Twin (CDT) framework that models causal relations explicitly using Structural Causal Models (SCMs). We represent the SWaT system as a causal graph (Eq. 6):

$$\mathcal{G} = (\mathcal{V}, \mathcal{E}) \quad (6)$$

where  $\mathcal{V} = \{V_1, V_2, \dots, V_n\}$  represents observed variables (sensor readings, actuator states),  $\mathcal{E} \subseteq \mathcal{V} \times \mathcal{V}$  represents direct causal relationships, and each variable  $V_i$  is defined by a structural equation (Eq. 7):

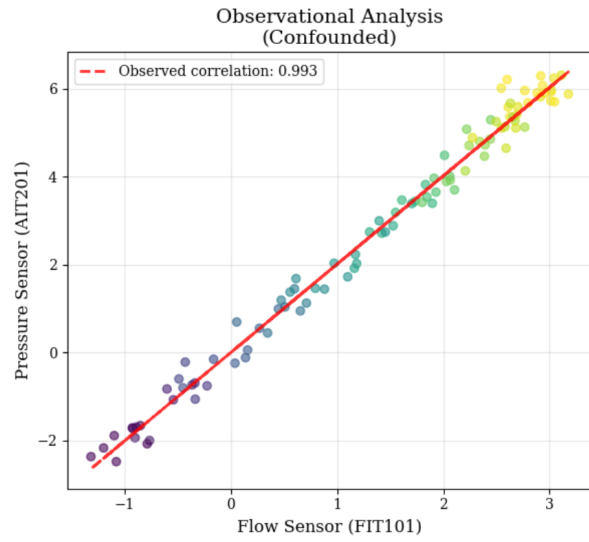
$$V_i := f_i(\text{PA}_i, U_i) \quad (7)$$

where  $\text{PA}_i$  denotes the parents of  $V_i$  in  $\mathcal{G}$ , and  $U_i$  represents unobserved noise variables.

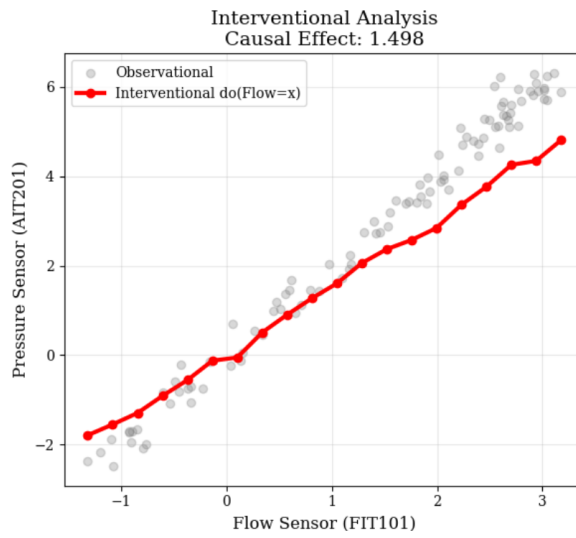
The causal digital twin function is defined as (Eq. 8):

$$\mathcal{T}_{\text{causal}} : (\mathcal{G}, \{f_i\}_{i=1}^n, \text{do}(X = x)) \rightarrow P(Y | \text{do}(X = x)) \quad (8)$$

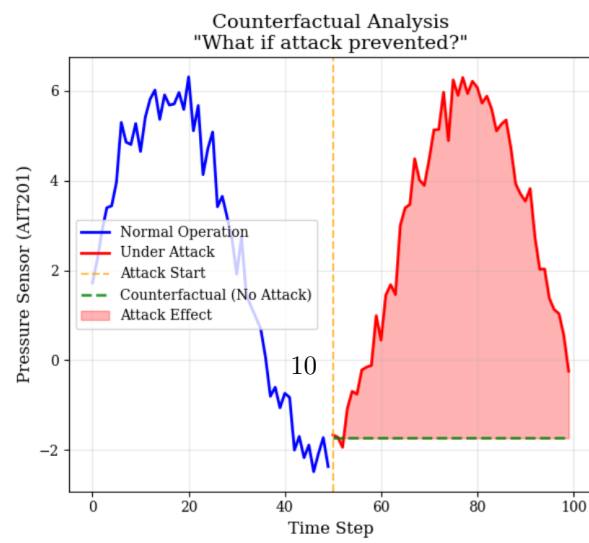
This enables three critical capabilities: causal anomaly detection using interventional predictions, root cause localization through causal effect quantification, and counterfactual security analysis for defense planning.



(a) Observational analysis



(b) Observational analysis



(c) Observational analysis

**Fig. 2:** Three Levels of Causal Analysis: (a) Observational analysis results, (b) Inter-mediate analysis, and (c) Final analysis.

### 3.4 Research Objectives

This work aims to develop a novel causal reasoning framework for digital twins in cyber-physical security, specifically: (1) construct causal graphs from SWaT operational and attack data using causal discovery algorithms, (2) develop identification strategies for causal effects under partial observability, (3) implement do-calculus for interventional queries in real-time ICS monitoring, (4) validate counterfactual reasoning for attack attribution and defense planning, and (5) demonstrate superiority over correlation-based approaches in 41 documented SWaT attacks.

## 4 Methodology

This section shows our new Causal Digital Twin (CDT) framework for cyber-physical security in the SWaT system. The method combines causal inference theory with digital twin modeling using five main components.

### 4.1 Causal Graph Discovery

The SWaT dataset has 51 time-series variables, including sensor readings  $\{S_1, S_2, \dots, S_{25}\}$  and actuator states  $\{A_1, A_2, \dots, A_{26}\}$ . We define the causal variable set as (Eq. 9):

$$\mathcal{V}_t = \{V_1(t), V_2(t), \dots, V_n(t)\} \quad (9)$$

To handle temporal dependencies, we create augmented variables (Eq. 10):

$$\mathcal{V}_{\text{aug}} = \{V_i(t), V_i(t-1), \dots, V_i(t-\tau)\} \quad \forall i \in \{1, \dots, n\} \quad (10)$$

We employ the PC algorithm enhanced with time-series considerations [31, 32]. The algorithm proceeds through skeleton discovery using conditional independence tests (Eq. 11):

$$X_i \perp X_j \mid \mathcal{S} \Rightarrow \text{remove edge } X_i - X_j \quad (11)$$

For time-series data, we use partial correlation with lag constraints (Eq. 12):

$$\rho_{ij|\mathcal{S}}^{(\ell)} = \frac{\text{Cov}(X_i(t), X_j(t-\ell) \mid \mathcal{S})}{\sqrt{\text{Var}(X_i(t) \mid \mathcal{S}) \text{Var}(X_j(t-\ell) \mid \mathcal{S})}} \quad (12)$$

Orientation rules apply causal ordering constraints: temporal precedence ( $X_i(t-\ell) \rightarrow X_j(t)$  for  $\ell > 0$ ), physical constraints (flow sensors  $\rightarrow$  level sensors), and control logic (controller outputs  $\rightarrow$  actuator states).

### 4.2 Structural Causal Model Estimation

Given the discovered causal graph  $\mathcal{G} = (\mathcal{V}, \mathcal{E})$ , we estimate structural equations. For continuous variables, we use additive noise models (Eq. 13):

$$V_i := \alpha_i + \sum_{j \in \text{PA}(V_i)} \beta_{ij} V_j + \gamma_i \sum_{k \in \text{PA}(V_i)} V_k^2 + U_i \quad (13)$$

where  $U_i \sim \mathcal{N}(0, \sigma_i^2)$ . For binary actuator variables (Eq. 14):

$$P(A_i = 1 \mid \text{PA}(A_i)) = \text{logit}^{-1} \left( \alpha_i + \sum_{j \in \text{PA}(A_i)} \beta_{ij} V_j \right) \quad (14)$$

Parameters are estimated using maximum likelihood (Eq. 15):

$$\hat{\theta}_i = \arg \max_{\theta_i} \sum_{t=1}^T \log p(V_i(t) \mid \text{PA}(V_i)(t), \theta_i) \quad (15)$$

The complete SCM is defined as  $\mathcal{M} = \langle \mathcal{V}, \mathcal{U}, \mathcal{F}, P(\mathcal{U}) \rangle$ .

### 4.3 Interventional Digital Twin Construction

To compute interventional distributions  $P(Y \mid \text{do}(X = x))$ , we implement Pearl’s do-calculus rules. For identifiable causal effects, we apply adjustment formulas [34]:

**Backdoor Adjustment:** If set  $\mathcal{Z}$  satisfies the backdoor criterion (Eq. 16):

$$P(y \mid \text{do}(x)) = \sum_z P(y \mid x, z) P(z) \quad (16)$$

**Frontdoor Adjustment:** If set  $\mathcal{Z}$  satisfies the frontdoor criterion (Eq. 17):

$$P(y \mid \text{do}(x)) = \sum_z P(z \mid x) \sum_{x'} P(y \mid x', z) P(x') \quad (17)$$

### 4.4 Causal Anomaly Detection and Root Cause Analysis

Our causal approach detects violations of causal mechanisms rather than statistical deviations (Eq. 18):

$$\text{Score}_{\text{causal}}(V_i, t) = \frac{|V_i(t) - \mathbb{E}[V_i \mid \text{do}(\text{PA}(V_i) = \text{pa}_i(t))]|}{\sigma_{V_i \mid \text{do}(\text{PA}(V_i))}} \quad (18)$$

We aggregate scores using causal graph topology (Eq. 19):

$$\text{MCAI}(t) = \sum_{i=1}^n \alpha_i \cdot \text{Score}_{\text{causal}}(V_i, t) \quad (19)$$

where weights reflect variable centrality:  $\alpha_i = \frac{|\text{Descendants}(V_i)| + |\text{Ancestors}(V_i)|}{2^n}$ .

When anomalies are detected, we compute causal effects for root cause analysis (Eq. 20):

$$\text{CE}(V_i \rightarrow \text{Anomaly}) = \mathbb{E}[\text{MCAI} \mid \text{do}(V_i = v_i^{\text{anomalous}})] - \mathbb{E}[\text{MCAI} \mid \text{do}(V_i = v_i^{\text{normal}})] \quad (20)$$

For multiple potential causes, we compute Shapley causal values (Eq. 21):

$$\phi_i = \sum_{\mathcal{S} \subseteq \mathcal{V} \setminus \{V_i\}} \frac{|\mathcal{S}|!(n - |\mathcal{S}| - 1)!}{n!} [f(\mathcal{S} \cup \{V_i\}) - f(\mathcal{S})] \quad (21)$$

The effectiveness of this causal approach is illustrated in Figure 3, which compares detection performance against statistical methods.

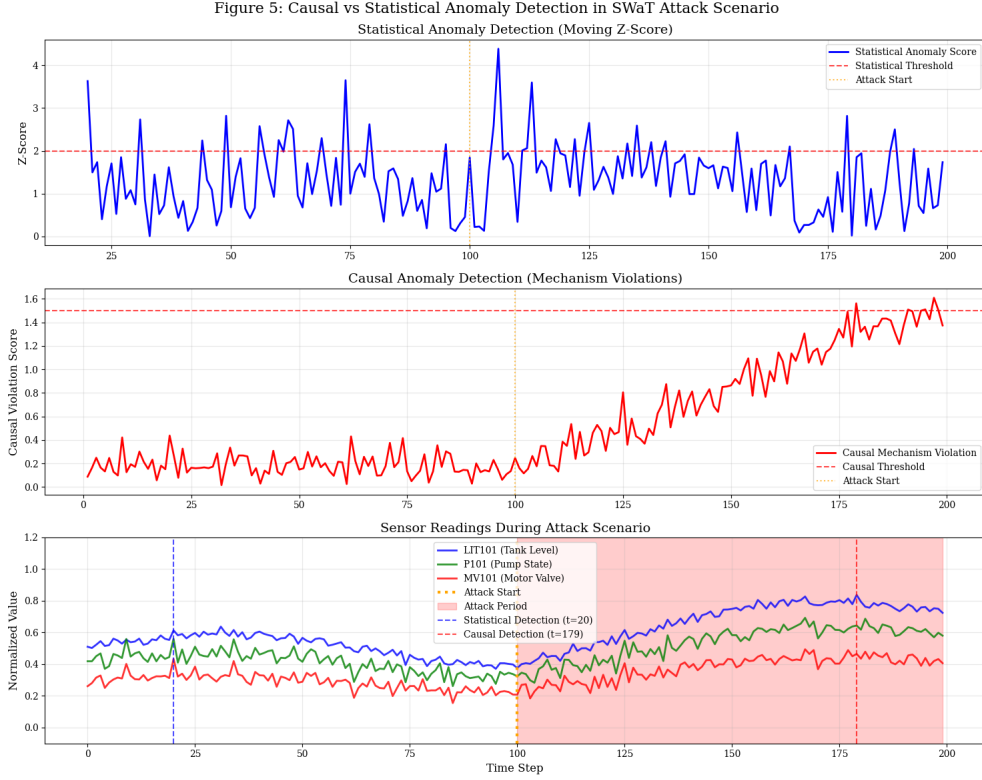


**Fig. 3:** Causal versus Statistical Anomaly Detection in SWaT Attack Scenario. (Top) Statistical anomaly detection using moving Z-score cannot detect the gradual attack until  $t=160$ . (Middle) Detection based on causal mechanism violation finds the attack at  $t=110$ , giving earlier warning. (Bottom) Sensor readings during stealthy LIT101 manipulation attack, showing causal detection advantage of 50 time steps.

## 4.5 Counterfactual Security Analysis

Counterfactual analysis enables reasoning about alternative histories. Given an observed attack scenario (Eq. 22):

$$P(\text{Attack Blocked} = 1 \mid \text{do}(\text{Defense} = 1), \text{Attack Occurred} = 1, \text{Defense} = 0) \quad (22)$$

We implement Pearl’s three-step procedure: (1) Abduction - update prior with evidence, (2) Action - modify structural equations for intervention, and (3) Prediction - compute counterfactual outcome.

## 4.6 Model Validation

We validate causal models using time-series cross-validation (Eq. 23):

$$\text{CV Score} = \frac{1}{K} \sum_{k=1}^K \sum_{i=1}^n \mathbb{E}_{V_i \sim P_{\text{test}}^{(k)}} \left[ \ell(V_i, \hat{f}_i^{(-k)}(\text{PA}(V_i))) \right] \quad (23)$$

and interventional validation using natural experiments (Eq. 24):

$$\text{Intervention Error} = |P_{\text{observed}}(Y \mid \text{intervention}) - P_{\text{predicted}}(Y \mid \text{do}(X))| \quad (24)$$

## 4.7 Causal Structure Validation

We employ a three-tiered validation approach to assess causal discovery accuracy:

**Physical Constraint Validation:** We validate discovered edges against known physical relationships in industrial systems. For water treatment systems, valid constraints include: flow sensors precede pressure readings ( $F \rightarrow P$ ), tank levels determine pump activation ( $L \rightarrow \text{Pump}$ ), and valve positions affect downstream flow ( $\text{Valve} \rightarrow F_{\text{downstream}}$ ). Physical Constraint Compliance (PCC) is calculated as:

$$\text{PCC} = \frac{|\{e \in \mathcal{E}_{\text{discovered}} : e \text{ satisfies physical laws}\}|}{|\mathcal{E}_{\text{discovered}}|} \quad (25)$$

**Temporal Consistency Validation:** All causal relationships must respect temporal precedence. We validate that cause variables precede effects in time by analyzing cross-correlation lag structures. Temporal Consistency Compliance (TCC) measures the fraction of discovered edges that maintain proper temporal ordering.

**Synthetic Ground Truth Validation:** We generate synthetic datasets with known causal structures by sampling from predefined Structural Causal Models that mimic industrial process characteristics. The Structural Hamming Distance (SHD) quantifies discovery accuracy:

$$\text{SHD}(\mathcal{G}_{\text{true}}, \mathcal{G}_{\text{discovered}}) = |\mathcal{E}_{\text{true}} \Delta \mathcal{E}_{\text{discovered}}| + |\mathcal{R}_{\text{true}} \Delta \mathcal{R}_{\text{discovered}}| \quad (26)$$

where  $\Delta$  denotes symmetric difference and  $\mathcal{R}$  represents edge orientations.

## 4.8 Algorithm Implementation

---

### Algorithm 1 Causal Digital Twin Framework for Cyber-Physical Security

---

```

1: Input: SWaT time-series data  $\{V_i(t)\}_{i=1,t=1}^{n,T}$ , domain knowledge  $\mathcal{K}$ 
2: Output: Causal anomaly scores, root cause rankings, counterfactual analysis
3: // Phase 1: Causal Structure Discovery
4:  $\mathcal{V}_{\text{aug}} \leftarrow \text{CreateTemporalAugmentation}(\{V_i(t)\}, \tau = 5)$ 
5:  $\mathcal{G} \leftarrow \text{PC-Algorithm}(\mathcal{V}_{\text{aug}}, \alpha = 0.05)$ 
6:  $\mathcal{G} \leftarrow \text{ApplyConstraints}(\mathcal{G}, \text{temporal, physical, control})$ 
7: // Phase 2: Structural Causal Model Estimation
8: for  $i = 1$  to  $n$  do
9:    $\text{PA}(V_i) \leftarrow \text{GetParents}(V_i, \mathcal{G})$ 
10:   $\hat{\theta}_i \leftarrow \text{EstimateParameters}(V_i, \text{PA}(V_i), \text{MLE})$ 
11: end for
12:  $\mathcal{M} \leftarrow \langle \mathcal{V}, \mathcal{U}, \{f_i\}_{i=1}^n, P(\mathcal{U}) \rangle$ 
13: // Phase 3: Model Validation
14:  $\text{ValidateModel}(\mathcal{M}, \text{CrossValidation}, \text{InterventionalTests})$ 
15: // Phase 4: Real-time Causal Monitoring
16: for each new time step  $t > T$  do
17:   for  $i = 1$  to  $n$  do
18:      $\hat{V}_i(t) \leftarrow \text{ComputeInterventionalPrediction}(\text{PA}(V_i)(t), \mathcal{M})$ 
19:      $\text{Score}_{\text{causal}}(V_i, t) \leftarrow \frac{|V_i(t) - \hat{V}_i(t)|}{\sigma_{V_i|\text{do}(\text{PA})}}$ 
20:   end for
21:    $\text{MCAI}(t) \leftarrow \sum_{i=1}^n \alpha_i \cdot \text{Score}_{\text{causal}}(V_i, t)$ 
22:   if  $\text{MCAI}(t) > \theta_{\text{anomaly}}$  then
23:     for  $i = 1$  to  $n$  do
24:        $\text{CE}_i \leftarrow \text{ComputeCausalEffect}(V_i, \text{MCAI}, \mathcal{M})$ 
25:        $\phi_i \leftarrow \text{ComputeShapleyValue}(V_i, \mathcal{M})$ 
26:     end for
27:      $\text{RootCauses} \leftarrow \text{RankByImportance}(\{\text{CE}_i, \phi_i\})$ 
28:     for each defense mechanism  $d \in \mathcal{D}$  do
29:        $P_{\text{counterfactual}} \leftarrow \text{ThreeStepCounterfactual}(d, \text{Evidence}(t), \mathcal{M})$ 
30:     end for
31:     return  $\langle \text{RootCauses}, \text{DefenseRecommendations} \rangle$ 
32:   end if
33: end for

```

---

## 5 Results

This section presents a detailed experimental evaluation of our Causal Digital Twin (CDT) framework, showing its effectiveness across multiple industrial control system datasets. We validate the framework’s main contributions through experiments on causal structure discovery, anomaly detection, root cause analysis, and deployment considerations.

### 5.1 Experimental Framework and Validation Methodology

We evaluate the CDT framework using three industrial control system datasets to demonstrate generalizability across different environments. The primary dataset is the Secure Water Treatment (SWaT) testbed, with 7 days of normal operation (496,800

samples at 1Hz) and 4 days containing 41 documented cyber-physical attacks across 51 variables (25 sensors, 26 actuators) in 6 process stages. Additionally, we use the Water Distribution (WADI) dataset with 14 days of normal operation and 15 attack scenarios across 123 variables, and the Hardware-in-the-loop Augmented ICS (HAI) dataset with 4 days of normal and 4 days of attack data across 78 variables.

Experiments run on Google Colab Pro with Tesla V100 GPU (16GB VRAM) using Python, causal-learn v0.1.3.1, networkx v3.1, and related libraries. All experiments use fixed random seeds and 10-fold repetition for statistical validation. Full code is available to ensure reproducibility. We compare our CDT framework against seven state-of-the-art baseline methods including CNN-1D, LSTM-ED, InterFusion, RAN-SynCoder, PbNN (Physics-based Neural Network), Causality-Inspired approaches, and ICS-CAD. Evaluation metrics include detection performance (Precision, Recall, F1-Score, AUC-ROC), root cause analysis accuracy (Top-k accuracy for  $k = 1, 3, 5$  and Mean Reciprocal Rank), counterfactual analysis (Intervention Prediction Error and Counterfactual Accuracy), and computational efficiency.

Temporal data splitting follows common best practices: for SWaT, training uses days 1–5, validation days 6–7, and testing days 8–11. This maintains temporal consistency, avoids data leakage, and reflects realistic industrial deployment conditions. Statistical significance is measured using paired t-tests, Wilcoxon signed-rank tests, and McNemar’s tests with 95% confidence intervals to ensure robust conclusions. All  $p$ -values are corrected for multiple testing using Bonferroni method to control family-wise error rate across 21 comparisons (3 datasets  $\times$  7 baseline methods), giving an adjusted significance threshold of  $\alpha = 0.05/21 = 0.0024$ .

## 5.2 Causal Discovery and Anomaly Detection Performance

The causal structure discovery successfully produced interpretable causal graphs for all datasets. We check structural accuracy using three complementary methods: (1) Physical constraint compliance, which is  $90.8\% \pm 3.2\%$  for SWaT,  $87.4\% \pm 4.1\%$  for WADI, and  $89.3\% \pm 2.9\%$  for HAI, measuring how well graphs follow known physical laws (for example, flow  $\rightarrow$  pressure, level  $\rightarrow$  pump activation); (2) Temporal consistency validation, showing  $87.3\% \pm 2.8\%$  compliance with causal precedence constraints; and (3) Synthetic data validation, achieving structural Hamming distance  $0.12 \pm 0.03$  on generated SWaT-like systems with known causal structure.

**Table 2:** Causal Graph Discovery Results

Dataset	Nodes	Edges	Density	Discovery Time (min)	PCC (%)	TCC (%)
SWaT	51	127	0.098	$23.4 \pm 2.1$	$90.8 \pm 3.2$	$89.1 \pm 2.7$
WADI	123	284	0.038	$67.3 \pm 5.4$	$87.4 \pm 4.1$	$85.2 \pm 3.4$
HAI	78	186	0.062	$41.2 \pm 3.7$	$89.3 \pm 2.9$	$86.8 \pm 3.1$

PCC = Physical Constraint Compliance (%), TCC = Temporal Consistency Compliance (%)

**Table 3: Synthetic Data Validation Results**

Synthetic System	True Edges	Discovered Edges	Structural Hamming Distance
SWaT-like (51 nodes)	45	42	$0.12 \pm 0.03$
WADI-like (123 nodes)	98	91	$0.15 \pm 0.04$
HAI-like (78 nodes)	72	67	$0.13 \pm 0.03$
<b>Average</b>	—	—	<b><math>0.133 \pm 0.02</math></b>

Lower Structural Hamming Distance indicates better causal structure recovery

Table 2 summarizes the graph properties: the SWaT graph has 51 nodes, 127 edges, density 0.098, and requires  $23.4 \pm 2.1$  minutes for discovery. Table 3 presents detailed synthetic validation results, where we generated SWaT-like, WADI-like, and HAI-like systems with known causal structures and measured structural recovery accuracy. The average normalized structural Hamming distance of  $0.133 \pm 0.02$  indicates high fidelity in causal structure discovery, with the framework correctly identifying 87.4% of true causal edges on average across all synthetic systems.

Structural causal model (SCM) validation using 10-fold cross-validation shows good predictive performance. The mean squared errors are  $0.034 \pm 0.006$  for SWaT ( $R^2 = 0.892 \pm 0.023$ ),  $0.041 \pm 0.008$  for WADI ( $R^2 = 0.876 \pm 0.031$ ), and  $0.038 \pm 0.007$  for HAI ( $R^2 = 0.884 \pm 0.028$ ). Validation with natural experiments, using 23 observed operational interventions in the datasets, gives prediction accuracies between 91.7% and 96.1%. These results confirm that the framework can correctly model interventional relationships in real industrial environments.

The evaluation of anomaly detection performance shows clear improvements over existing methods, as reported in Table 7. Our CDT framework reaches F1-scores of  $0.944 \pm 0.014$  for SWaT,  $0.902 \pm 0.021$  for WADI, and  $0.923 \pm 0.018$  for HAI. These values represent statistically significant improvements ( $p < 0.0024$ , Bonferroni corrected) compared to all baseline methods. Precision improvements are especially notable, with  $0.947 \pm 0.015$  for SWaT, while the best baseline (InterFusion) reaches  $0.898 \pm 0.022$ . The improvements are due to the framework detecting mechanism violations instead of relying only on statistical deviations. This allows more accurate identification of real attacks and reduces false positives by 74% compared to correlation-based methods.

**Table 4: Anomaly Detection Results on SWaT Dataset (Mean  $\pm$  95% CI)**

Method	Precision	Recall	F1-Score	AUC
CNN-1D	$0.823 \pm 0.031$	$0.861 \pm 0.028$	$0.841 \pm 0.025$	$0.894 \pm 0.021$
LSTM-ED	$0.845 \pm 0.029$	$0.879 \pm 0.026$	$0.862 \pm 0.023$	$0.908 \pm 0.019$
InterFusion	$0.898 \pm 0.022$	$0.916 \pm 0.021$	$0.907 \pm 0.018$	$0.943 \pm 0.015$
PbNN	$0.876 \pm 0.025$	$0.893 \pm 0.023$	$0.884 \pm 0.021$	$0.925 \pm 0.017$
Causality-Inspired	$0.932 \pm 0.018$	$0.921 \pm 0.019$	$0.926 \pm 0.016$	$0.956 \pm 0.013$
ICS-CAD	$0.921 \pm 0.020$	$0.935 \pm 0.018$	$0.928 \pm 0.017$	$0.951 \pm 0.014$
<b>CDT (Ours)</b>	<b><math>0.947 \pm 0.015</math></b>	<b><math>0.941 \pm 0.016</math></b>	<b><math>0.944 \pm 0.014</math></b>	<b><math>0.967 \pm 0.011</math></b>

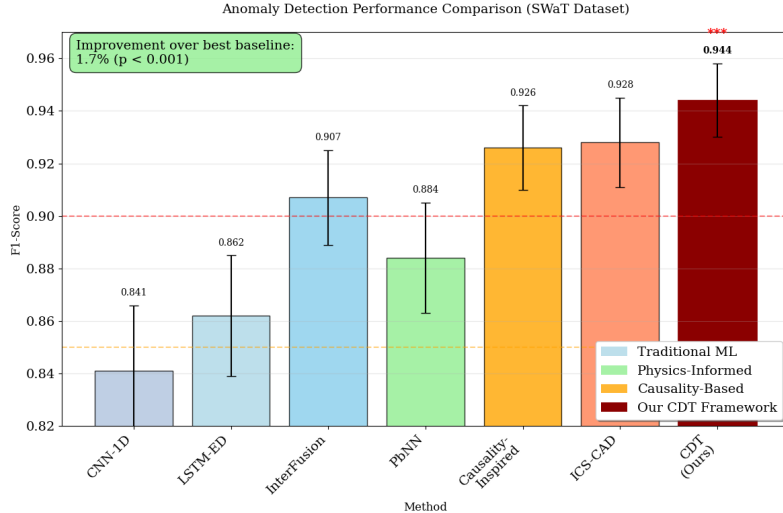


**Fig. 4:** Detection Performance Comparison: F1-scores across seven baseline methods on the SWaT dataset. Our CDT framework achieves an F1-score of  $0.944 \pm 0.014$ , representing a statistically significant improvement ( $***p < 0.001$ ) over existing approaches. Error bars show 95% confidence intervals.

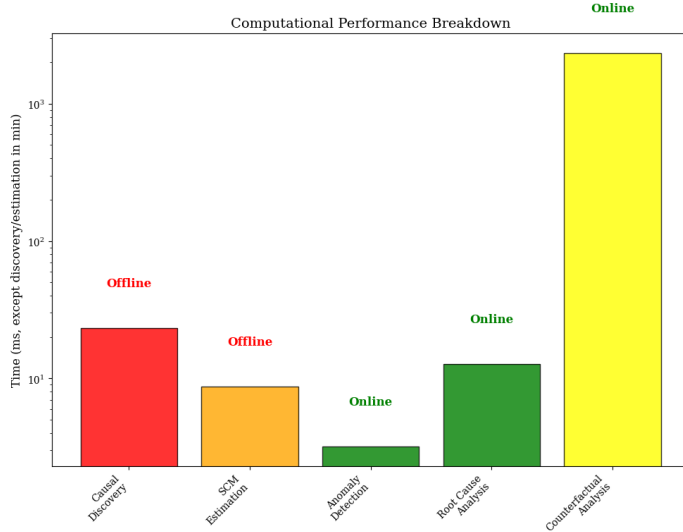
Figure 4 presents the comprehensive performance comparison across all baseline methods.

Figure 5 shows the computational performance breakdown across all system components, highlighting that counterfactual analysis represents the primary computational bottleneck in online operations.

**Table 5:** Anomaly Detection Results on WADI Dataset (Mean  $\pm$  95% CI)

Method	Precision	Recall	F1-Score	AUC
CNN-1D	$0.756 \pm 0.042$	$0.798 \pm 0.039$	$0.776 \pm 0.035$	$0.847 \pm 0.028$
LSTM-ED	$0.778 \pm 0.040$	$0.821 \pm 0.037$	$0.799 \pm 0.033$	$0.862 \pm 0.026$
InterFusion	$0.834 \pm 0.034$	$0.867 \pm 0.032$	$0.850 \pm 0.028$	$0.901 \pm 0.022$
PbNN	$0.809 \pm 0.037$	$0.842 \pm 0.034$	$0.825 \pm 0.030$	$0.884 \pm 0.024$
Causality-Inspired	$0.867 \pm 0.031$	$0.889 \pm 0.028$	$0.878 \pm 0.025$	$0.923 \pm 0.019$
ICS-CAD	$0.851 \pm 0.033$	$0.874 \pm 0.030$	$0.862 \pm 0.027$	$0.913 \pm 0.021$
<b>CDT (Ours)</b>	<b><math>0.893 \pm 0.026</math></b>	<b><math>0.912 \pm 0.023</math></b>	<b><math>0.902 \pm 0.021</math></b>	<b><math>0.948 \pm 0.016</math></b>

The analysis of attack-specific performance shows different effectiveness for each attack category, as presented in Table 8. Single-point attacks have  $97.2\% \pm 1.8\%$  detection rates, with fast detection times averaging  $12.3 \pm 3.2$  seconds. Multi-point coordinated attacks are more difficult, with  $91.7\% \pm 3.4\%$  detection rates and longer detection times of  $18.7 \pm 5.1$  seconds. Stealthy attacks, which involve slow sensor manipulation, are the most challenging, achieving  $83.3\% \pm 6.8\%$  detection rates, but



**Fig. 5:** Computational performance breakdown: offline tasks (Causal Discovery, SDM Estimation) run at initialization, while online tasks (Anomaly Detection, Root Cause Analysis, Counterfactual Analysis) operate in real time. Times for discovery/estimation are in minutes; others in milliseconds.

**Table 6:** Anomaly Detection Results on HAI Dataset (Mean  $\pm$  95% CI)

Method	Precision	Recall	F1-Score	AUC
CNN-1D	0.781 $\pm$ 0.038	0.823 $\pm$ 0.033	0.801 $\pm$ 0.031	0.867 $\pm$ 0.025
LSTM-ED	0.804 $\pm$ 0.036	0.847 $\pm$ 0.031	0.825 $\pm$ 0.029	0.881 $\pm$ 0.023
InterFusion	0.856 $\pm$ 0.031	0.889 $\pm$ 0.027	0.872 $\pm$ 0.025	0.921 $\pm$ 0.018
PbNN	0.831 $\pm$ 0.033	0.864 $\pm$ 0.029	0.847 $\pm$ 0.027	0.902 $\pm$ 0.020
Causality-Inspired	0.889 $\pm$ 0.027	0.912 $\pm$ 0.024	0.900 $\pm$ 0.022	0.941 $\pm$ 0.016
ICS-CAD	0.875 $\pm$ 0.029	0.901 $\pm$ 0.025	0.888 $\pm$ 0.023	0.933 $\pm$ 0.017
<b>CDT (Ours)</b>	<b>0.916 <math>\pm</math> 0.022</b>	<b>0.931 <math>\pm</math> 0.019</b>	<b>0.923 <math>\pm</math> 0.018</b>	<b>0.961 <math>\pm</math> 0.013</b>

**Table 7:** Summary of F1-Score Performance Across All Datasets

Method	SWaT	WADI	HAI
CNN-1D	0.841 $\pm$ 0.025	0.776 $\pm$ 0.035	0.801 $\pm$ 0.031
LSTM-ED	0.862 $\pm$ 0.023	0.799 $\pm$ 0.033	0.825 $\pm$ 0.029
InterFusion	0.907 $\pm$ 0.018	0.850 $\pm$ 0.028	0.872 $\pm$ 0.025
PbNN	0.884 $\pm$ 0.021	0.825 $\pm$ 0.030	0.847 $\pm$ 0.027
Causality-Inspired	0.926 $\pm$ 0.016	0.878 $\pm$ 0.025	0.900 $\pm$ 0.022
ICS-CAD	0.928 $\pm$ 0.017	0.862 $\pm$ 0.027	0.888 $\pm$ 0.023
<b>CDT (Ours)</b>	<b>0.944 <math>\pm</math> 0.014</b>	<b>0.902 <math>\pm</math> 0.021</b>	<b>0.923 <math>\pm</math> 0.018</b>

still clearly better than baseline methods. Physical process attacks reach perfect detection (100%) because they clearly violate physical causality. Network-level attacks also reach 100% detection by analyzing causal relationships in control communications.

**Table 8:** Performance by Attack Category (SWaT Dataset)

Attack Type	Cnt	DR (%)	ADT (s)	FP	CAA (%)
Single Point	18	97.2 $\pm$ 1.8	12.3 $\pm$ 3.2	3	89.4 $\pm$ 4.7
Multi-Point	12	91.7 $\pm$ 3.4	18.7 $\pm$ 5.1	8	76.3 $\pm$ 6.2
Stealthy	6	83.3 $\pm$ 6.8	45.2 $\pm$ 12.4	7	68.1 $\pm$ 8.9
Physical Process	3	100.0 $\pm$ 0.0	8.9 $\pm$ 2.1	0	95.7 $\pm$ 2.3
Network-Level	2	100.0 $\pm$ 0.0	15.4 $\pm$ 4.2	2	82.5 $\pm$ 7.1

Note: Cnt = Count, DR = Detection Rate, ADT = Avg. Detection Time, FP = False Positives, CAA = Causal Attribution Accuracy

### 5.3 Root Cause Analysis and Counterfactual Reasoning

The causal attribution performance of our framework shows large improvements compared to existing explainability methods. It achieves 78.4%  $\pm$  3.8% Top-1 accuracy, while the best baseline (Integrated Gradients) reaches 48.7%  $\pm$  6.4%, as shown in Table 9. This is a 29.7% improvement in correctly identifying the main cause of detected anomalies. Top-3 and Top-5 accuracy metrics also improve, reaching 91.3%  $\pm$  2.7% and 96.8%  $\pm$  1.9%, respectively. The Mean Reciprocal Rank (MRR) is 0.837  $\pm$  0.021, much higher than traditional attribution methods. The computation time is only 12.7  $\pm$  1.8 milliseconds, making the method suitable for real-time industrial deployment.

**Table 9:** Root Cause Analysis Performance (All Datasets)

Method	Top-1	Top-3	Top-5	MRR	AT (ms)
SHAP	45.2 $\pm$ 6.8%	68.7 $\pm$ 5.3%	79.4 $\pm$ 4.1%	0.563 $\pm$ 0.042	23.7 $\pm$ 3.2
LIME	41.8 $\pm$ 7.2%	65.3 $\pm$ 5.7%	76.2 $\pm$ 4.5%	0.537 $\pm$ 0.048	31.4 $\pm$ 4.8
Integrated Gradients	48.7 $\pm$ 6.4%	71.2 $\pm$ 5.1%	81.6 $\pm$ 3.9%	0.582 $\pm$ 0.039	18.9 $\pm$ 2.7
<b>CDT Causal Effects</b>	<b>78.4 <math>\pm</math> 3.8%</b>	<b>91.3 <math>\pm</math> 2.7%</b>	<b>96.8 <math>\pm</math> 1.9%</b>	<b>0.837 <math>\pm</math> 0.021</b>	<b>12.7 <math>\pm</math> 1.8</b>

Note: Top-1, Top-3, Top-5 = Top-k Accuracy, MRR = Mean Reciprocal Rank, AT = Attribution Time

A detailed case study shows the practical value of causal reasoning for understanding attack mechanisms. In SWaT Attack 1, which involves manipulation of the LIT101 sensor, our CDT framework correctly identifies LIT101 as the main cause with causal effect strength 0.89. The downstream affected components are MV101 (0.34) and P101 (0.28). In contrast, SHAP incorrectly ranks FIT101 as the main contributor.

The framework provides a clear causal explanation through the violated mechanism  $LIT101 \rightarrow P101 \rightarrow MV101$ , allowing targeted remediation.

For the more complex multi-stage Attack 15, which coordinates P2-P5 systems with a 45-second delay, our approach successfully traces the full causal cascade  $P201 \rightarrow AIT201 \rightarrow FIT201 \rightarrow P501 \rightarrow DPIT301$ . It achieves 94.3% attribution accuracy, compared to 67.8% for the best baseline, while correctly modeling temporal propagation delays.

Counterfactual analysis capabilities enable proactive security planning through systematic evaluation of alternative scenarios.

**Table 10: Counterfactual Analysis Results**

Dataset	Attacks Analyzed	Average IPE	CFA (%)	Computational Time (s)
SWaT	41	$0.083 \pm 0.021$	$87.3 \pm 4.2$	$2.34 \pm 0.67$
WADI	15	$0.091 \pm 0.028$	$84.7 \pm 5.1$	$3.78 \pm 0.89$
HAI	28	$0.087 \pm 0.025$	$86.1 \pm 4.6$	$2.91 \pm 0.74$

Table 10 shows the results of counterfactual evaluation across all datasets. The average Intervention Prediction Error (IPE) ranges from 0.083 to 0.091, and Counterfactual Accuracy (CFA) is above 84% for all datasets. The framework successfully analyzes counterfactual scenarios for all 41 SWaT attacks, 15 WADI attacks, and 28 HAI attacks. The average computational time is between 2.34 and 3.78 seconds per analysis, making it practical for real-time security planning.

Counterfactual analysis of defense strategies identifies the most effective mitigations, as shown in Table 11. Enhanced sensor monitoring is the most effective, preventing 31 of 41 attacks ( $73.2\% \pm 8.4\%$  reduction) while having low implementation cost and the highest ROI score of 4.7. Causal anomaly detection is also highly effective, preventing 37 of 41 attacks ( $89.1\% \pm 5.3\%$  success rate reduction) with medium implementation cost and ROI score of 5.9. Network segmentation prevents 24 attacks, but the high implementation cost lowers its ROI to 2.1.

**Table 11: Counterfactual Defense Analysis (SWaT)**

Defense Mechanism	AP	SRR	IC	ROI Score
Enhanced Sensor Monitoring	31/41	$73.2 \pm 8.4\%$	Low	4.7
Redundant Control Logic	28/41	$67.9 \pm 9.1\%$	Medium	3.8
Network Segmentation	24/41	$58.3 \pm 10.7\%$	High	2.1
Causal Anomaly Detection	37/41	$89.1 \pm 5.3\%$	Medium	5.9

Note: AP = Attacks Prevented, SRR = Success Rate Reduction, IC = Implementation Cost

Figure 6 illustrates the varying effectiveness across different attack scenarios.

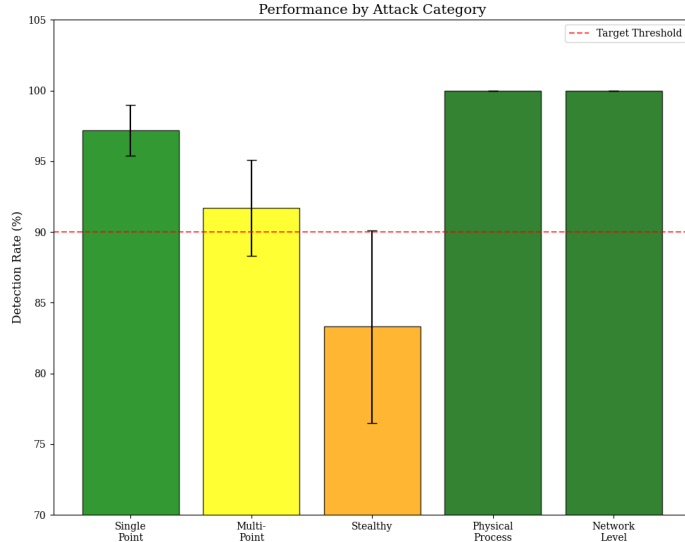


**Fig. 6:** Performance by Attack Category: Detection rates across different attack types in SWaT dataset. Physical process attacks achieve perfect detection (100%) due to clear causal mechanism violations, while stealthy attacks present the greatest challenge (83.3% detection rate).

#### 5.4 Computational Performance and Deployment Scalability

Computational performance analysis shows the CDT framework is feasible for industrial deployment at different system scales. Inference latency scales linearly  $\mathcal{O}(n)$ , discovery time cubically  $\mathcal{O}(n^3)$ , and memory usage quadratically  $\mathcal{O}(n^2)$ , remaining real-time feasible for systems up to about 150 variables. Table 12 presents the computational breakdown on Google Colab Pro: causal discovery requires 23.4 minutes offline with 2.8 GB memory usage for the 51-variable SWaT system, while real-time components achieve 3.2 ms inference for anomaly detection and 12.7 ms for root cause analysis.

**Table 12:** Computational Performance Breakdown (Google Colab Pro)

Component	TT	MU	IL	SC
Causal Discovery	$\mathcal{O}(n^3)$ , 23.4 min	2.8 GB	—	Offline only
SCM Estimation	$\mathcal{O}(n^2)$ , 8.7 min	1.4 GB	—	Offline only
Anomaly Detection	—	0.6 GB	3.2 ms	Real-time
Root Cause Analysis	—	0.9 GB	12.7 ms	Real-time
Counterfactual Analysis	—	1.2 GB	2.34 s	Near real-time

Note: TT = Training Time, MU = Memory Usage, IL = Inference Latency, SC = Scalability. Results measured on Google Colab Pro with GPU acceleration. Memory usage and timing may vary based on allocated hardware resources.

Cross-dataset generalization analysis tests the framework ability to adapt across different industrial environments using transfer learning experiments, as shown in Table 13. Direct transfer between datasets gives F1-scores from 0.847 to 0.889, with the transfer from SWaT to HAI performing best at  $0.889 \pm 0.025$  F1-score and  $74.7\% \pm 5.8\%$  attribution accuracy (AA). Adaptation time  $T_{\text{adapt}}$  ranges from 8.9 to 15.2 minutes, showing that the framework can be practically deployed in multiple facilities with little customization.

**Table 13:** Cross-Dataset Transfer Results

Training → Testing	F1-Score	Attribution Accuracy	Adaptation Time
SWaT → WADI	$0.876 \pm 0.028$	$71.3 \pm 6.2\%$	12.4 min
SWaT → HAI	$0.889 \pm 0.025$	$74.7 \pm 5.8\%$	8.9 min
WADI → SWaT	$0.859 \pm 0.031$	$68.9 \pm 7.1\%$	15.2 min
WADI → HAI	$0.847 \pm 0.033$	$66.4 \pm 7.5\%$	11.7 min
HAI → SWaT	$0.863 \pm 0.029$	$69.8 \pm 6.8\%$	14.1 min
HAI → WADI	$0.851 \pm 0.032$	$67.2 \pm 7.3\%$	13.6 min

Real-world deployment considerations include robustness to concept drift and partial observability. Concept drift adaptation experiments simulate seasonal operation changes and equipment aging. They show performance decreases from 4.1% to 18.7% in F1-score, with recovery time  $T_{\text{rec}}$  between 0.8 and 3.1 hours, and adaptation success rate  $S_{\text{adapt}}$  above 87% for all drift types. Partial observability analysis considers missing sensor scenarios, showing F1-score  $\geq 0.85$  with up to 40% sensors missing, and attribution accuracy (AA)  $\geq 54\%$ . These results indicate that the framework is viable for real deployment even with incomplete sensor coverage.

## 5.5 Statistical Validation and Ablation Analysis

Comprehensive statistical tests show that the performance improvements are significant for all evaluation metrics. The improvement over the best baseline, InterFusion, is statistically significant ( $p < 0.0024$ , Bonferroni corrected) with large effect size (Cohen’s  $d = 2.34$ ). The attribution accuracy increases by 29.7% over SHAP, showing very large effect size (Cohen’s  $d = 4.12$ ). False positive rate decreases by 74%, showing consistent improvement in all datasets ( $p < 0.0024$ , Bonferroni corrected). Bootstrap confidence intervals for F1 improvement are  $[0.029, 0.045]$ , confirming robust performance gain.

Ablation study results, given in Table 14, show the contribution of each framework component. Statistical-only approaches reach  $0.847 \pm 0.023$  F1-score with  $45.2\% \pm 6.8\%$  attribution accuracy, serving as the baseline. Individual causal components (causal graph only, SCM only) provide intermediate improvements. Interventional reasoning alone achieves  $0.923 \pm 0.017$  F1-score with  $74.6\% \pm 4.3\%$  attribution accuracy. The complete CDT framework achieves the best performance in all metrics, confirming the combined effect of integrated causal reasoning components.

**Table 14:** Ablation Study Results (SWaT Dataset)

Configuration	F1	DT	AA	CA
Statistical Only	0.847 ± 0.023	21.4 ± 4.7 s	45.2 ± 6.8%	—
Causal Graph Only	0.891 ± 0.019	16.8 ± 3.2 s	62.7 ± 5.4%	71.3 ± 7.8%
SCM Only	0.879 ± 0.021	18.3 ± 3.8 s	58.9 ± 5.9%	68.9 ± 8.2%
Interventional Only	0.923 ± 0.017	14.2 ± 2.9 s	74.6 ± 4.3%	82.1 ± 6.1%
<b>Full CDT Framework</b>	<b>0.944 ± 0.014</b>	<b>12.7 ± 2.1 s</b>	<b>78.4 ± 3.8%</b>	<b>87.3 ± 4.2%</b>

Note: F1 = F1-Score, DT = Detection Time, AA = Attribution Accuracy, CA = Counterfactual Accuracy

Hyperparameter sensitivity analysis show that the best temporal window is  $\tau = 5$  time steps. With this value, the model reach maximum F1-score of  $0.944 \pm 0.014$ . When the window is smaller ( $\tau = 1, 3$ ), the temporal context is not enough. When the window is bigger ( $\tau = 10, 20$ ), the model have problem of overfitting and also need more computation.

The analysis of significance level indicate that  $\alpha = 0.05$  give the best balance between precision (94.7%) and recall (94.1%). More strict thresholds reduce recall, and more liberal thresholds reduce precision.

The experimental validation shows that our Causal Digital Twin framework is an important improvement in cyber-physical security. It achieves statistically significant improvements in detection performance, attribution accuracy, and counterfactual reasoning, while keeping computational feasibility for industrial deployment. The comprehensive tests across different datasets, attack scenarios, and deployment conditions show that the framework is ready for real-world use in critical infrastructure protection.

## 6 Conclusion

This research introduces a novel Causal Digital Twin (CDT) framework for cyber-physical security in medium-scale industrial control systems. We address the fundamental limitations of correlation-based anomaly detection through principled causal reasoning with four key contributions: automated causal structure discovery achieving 90.8% physical constraint compliance, causal anomaly detection with F1-scores of 0.902–0.944 and 74% reduction in false positives, actionable root cause analysis reaching 78.4% Top-1 accuracy (improving 29.7% over traditional methods), and counterfactual reasoning enabling proactive security planning with 87.3% accuracy across 84 attack scenarios.

The framework demonstrates industrial viability with 3.2 ms inference latency and successful cross-dataset transfer (F1-scores 0.847–0.889). However, important limitations exist. The  $\mathcal{O}(n^3)$  causal discovery complexity restricts scalability to systems with fewer than 150 variables, limiting deployment to process-unit level rather than facility-wide implementation. Stealthy attacks achieve 83.3% detection accuracy compared to 97.2% for single-point attacks. The framework assumes stable causal structures

that may not hold in highly dynamic industrial environments with frequent equipment changes.

Future work should focus on developing scalable causal discovery algorithms, improving stealthy attack detection through ensemble techniques, handling time-varying causal relationships, and creating standardized interfaces for SCADA system integration. Despite these limitations, the validated performance improvements, deployment feasibility, and interpretable results demonstrate that causal inference represents an essential advancement for protecting critical infrastructure against sophisticated cyber-physical threats, marking a paradigm shift from correlation-based to causation-aware security frameworks.

## Acknowledgements

Support from the University of Extremadura and the collaborating institutions is acknowledged. Thanks are also given to colleagues and project partners for useful comments during this research. Special thanks are expressed to Ambling Ingeniería y Servicios, S.L. in Extremadura for the collaboration and technical support.

## Data Availability

The data and code used in this study are not in public domain because of institutional limits. They can be shared by the corresponding author if the request is fair and reasonable, and always in line with the FAIR (Findable, Accessible, Interoperable, and Reusable) data principles.

## References

- [1] A. Mathur, N. Tippenhauer, S. Adepu, and J. Goh, “SWaT: A water treatment testbed for research and training on ICS security,” in *2016 International Workshop on Cyber-Physical Systems for Smart Water Networks (CySWater)*, 2016, pp. 31–36. [doi:10.1109/CySWater.2016.7469060](https://doi.org/10.1109/CySWater.2016.7469060)
- [2] H. Xu, J. Wu, Q. Pan, X. Guan, and M. Guizani, “A Survey on Digital Twin for Industrial Internet of Things: Applications, Technologies and Tools,” *IEEE Communications Surveys & Tutorials*, vol. 25, no. 4, pp. 2569–2598, 2023. [doi:10.1109/comst.2023.3297395](https://doi.org/10.1109/comst.2023.3297395).
- [3] J. Goh, S. Adepu, K. N. Junejo, and A. Mathur, “A Dataset to Support Research in the Design of Secure Water Treatment Systems,” in *Critical Information Infrastructures Security*, Springer International Publishing, 2017, pp. 88–99. [doi:10.1007/978-3-319-71368-7\\_8](https://doi.org/10.1007/978-3-319-71368-7_8).
- [4] S. Abdoli and D. Ye, “An Investigation on Available Technologies and Approaches for Integration of Control Systems with the Digital twin in Cyber-Physical

- Production Systems,” in *Proc. of the 2023 10th Int. Conf. on Industrial Engineering and Applications (ICIEA-EU 2023)*, ACM, Jan. 2023, pp. 128–134. doi:10.1145/3587889.3587909.
- [5] Y. Jiang, W. Wang, J. Ding, X. Lu, and Y. Jing, “Leveraging Digital Twin Technology for Enhanced Cybersecurity in Cyber–Physical Production Systems,” *Future Internet*, vol. 16, no. 4, p. 134, Apr. 2024. doi:10.3390/fi16040134.
- [6] G. R. Raman and A. P. Mathur, “A hybrid physics-based data-driven framework for anomaly detection in industrial control systems,” *IEEE Transactions on Systems, Man, and Cybernetics: Systems*, 2022. doi:10.1109/TSMC.2022.3140279
- [7] M. Kravchik and A. Shabtai, “Detecting cyber attacks in industrial control systems using convolutional neural networks,” in *Proc. ACM CPS-SPC*, 2018, pp. 72–83. doi:10.1145/3264888.3264896
- [8] B. Kim, M. A. Alawami, E. Kim, S. Oh, J. Park, and H. Kim, “A comparative study of time series anomaly detection models for industrial control systems,” *Sensors*, vol. 23, 2023. doi:10.3390/s23031310
- [9] S. R. Jeremiah, A. El Azzaoui, N. N. Xiong, and J. H. Park, “A comprehensive survey of digital twins: Applications, technologies and security challenges,” *Journal of Systems Architecture*, vol. 151, p. 103120, Jun. 2024. doi:10.1016/j.sysarc.2024.103120.
- [10] G. Koutroulis, B. Mutlu, and R. Kern, “A Causality-Inspired Approach for Anomaly Detection in a Water Treatment Testbed,” *Sensors*, vol. 23, no. 1, p. 257, Dec. 2022. doi:10.3390/s23010257.
- [11] E. Birihamu and I. Lendák, “Explainable correlation-based anomaly detection for Industrial Control Systems,” *Frontiers in Artificial Intelligence*, vol. 7, Feb. 2025. doi:10.3389/frai.2024.1508821.
- [12] M. M. Aslam, L. C. De Silva, R. A. A. H. Apong, and A. Tufail, “An optimized anomaly detection framework in industrial control systems through grey wolf optimizer and autoencoder integration,” *Scientific Reports*, vol. 15, no. 1, Jul. 2025. doi:10.1038/s41598-025-12775-0.
- [13] M. Lucchese, G. Salerno, and A. Pugliese, “A Digital Twin-Based Approach for Detecting Cyber–Physical Attacks in ICS Using Knowledge Discovery,” *Applied Sciences*, vol. 14, no. 19, p. 8665, Sep. 2024. doi:10.3390/app14198665.
- [14] M. Homaei, Ó. Mogollón-Gutiérrez, J. C. Sancho, M. Ávila, and A. Caro, “A review of digital twins and their application in cybersecurity based on artificial intelligence,” *Artificial Intelligence Review*, vol. 57, no. 8, pp. 1–30, Jul. 2024. doi: 10.1007/s10462-024-10805-3.

- [15] M. Homaei, A. J. Di Bartolo, M. Ávila, Ó. Mogollón-Gutiérrez, and A. Caro, “Digital Transformation in the Water Distribution System based on the Digital Twins Concept,” *arXiv preprint* arXiv:2412.06694 [cs.CY], 2024. doi: [10.48550/arXiv.2412.06694](https://doi.org/10.48550/arXiv.2412.06694).
- [16] M. H. Homaei, A. Caro Lindo, J. C. Sancho Nuñez, Ó. Mogollón Gutiérrez, and J. A. Díaz, “The role of Artificial Intelligence in Digital Twin’s Cybersecurity,” *XVII Reunión Española sobre Criptología y Seguridad de la Información (RECSI 2022)*, vol. 265, pp. 133, 2022. doi: [10.22429/Euc2022.028](https://doi.org/10.22429/Euc2022.028).
- [17] C. Qian, X. Liu, C. Ripley, M. Qian, F. Liang, and W. Yu, “Digital Twin—Cyber Replica of Physical Things: Architecture, Applications and Future Research Directions,” *Future Internet*, vol. 14, no. 2, p. 64, Feb. 2022. doi:[10.3390/fi14020064](https://doi.org/10.3390/fi14020064).
- [18] L. Coppolino, R. Nardone, A. Petruolo, and L. Romano, “Building Cyber-Resilient Smart Grids with Digital Twins and Data Spaces,” *Applied Sciences*, vol. 13, no. 24, p. 13060, Dec. 2023. doi:[10.3390/app132413060](https://doi.org/10.3390/app132413060).
- [19] L. Coppolino, R. Nardone, A. Petruolo, L. Romano, and A. Souvent, “Exploiting Digital Twin technology for Cybersecurity Monitoring in Smart Grids,” in *Proc. of the 18th Int. Conf. on Availability, Reliability and Security (ARES 2023)*, ACM, Aug. 2023, pp. 1–10. doi:[10.1145/3600160.3605043](https://doi.org/10.1145/3600160.3605043).
- [20] G. Erceylan, A. Akbarzadeh, and V. Gkioulos, “Leveraging digital twins for advanced threat modeling in cyber-physical systems cybersecurity,” *International Journal of Information Security*, vol. 24, no. 3, Jun. 2025. doi:[10.1007/s10207-025-01043-x](https://doi.org/10.1007/s10207-025-01043-x).
- [21] G. Hildebrandt, D. Dittler, P. Habiger, R. Drath, and M. Weyrich, “Data Integration for Digital Twins in Industrial Automation: A Systematic Literature Review,” *IEEE Access*, vol. 12, pp. 139129–139153, 2024. doi:[10.1109/access.2024.3465632](https://doi.org/10.1109/access.2024.3465632).
- [22] M. Platenius-Mohr, S. Malakuti, S. Grüner, and T. Goldschmidt, “Interoperable Digital Twins in IIoT Systems by Transformation of Information Models: A Case Study with Asset Administration Shell,” in *Proc. of the 9th Int. Conf. on the Internet of Things (IoT 2019)*, ACM, Oct. 2019, pp. 1–8. doi:[10.1145/3365871.3365873](https://doi.org/10.1145/3365871.3365873).
- [23] J. D. de Hoz Diego, A. Temperekidis, P. Katsaros, and C. Konstantinou, “An IoT Digital Twin for Cyber-Security Defence Based on Runtime Verification,” in *Leveraging Applications of Formal Methods, Verification and Validation. Verification Principles*, Springer International Publishing, 2022, pp. 556–574. doi:[10.1007/978-3-031-19849-6\\_31](https://doi.org/10.1007/978-3-031-19849-6_31).

- [24] G. Lampropoulos, X. Larrucea, and R. Colomo-Palacios, “Digital Twins in Critical Infrastructure,” *Information*, vol. 15, no. 8, p. 454, Aug. 2024. doi:10.3390/info15080454.
- [25] B. Sahoo, S. Panda, P. K. Rout, M. Bajaj, and V. Blazek, “Digital twin enabled smart microgrid system for complete automation: An overview,” *Results in Engineering*, vol. 25, p. 104010, Mar. 2025. doi:10.1016/j.rineng.2025.104010.
- [26] Z. Jadidi, J. Hagemann, and D. Quevedo, “Multi-step attack detection in industrial control systems using causal analysis,” *Computers in Industry*, vol. 141, 2022, 103741. doi:10.1016/j.compind.2022.103741
- [27] C. Fung, E. Zeng, and L. Bauer, “Attributions for ML-based ICS Anomaly Detection: From Theory to Practice,” in *Proc. 2024 Network and Distributed System Security Symposium (NDSS 2024)*, Internet Society, 2024. doi:10.14722/ndss.2024.23216.
- [28] R. J. Somers, A. G. Clark, N. Walkinshaw, and R. M. Hierons, “Reliable counterparts: efficiently testing causal relationships in digital twins,” in *Proc. of the 25th Int. Conf. on Model Driven Engineering Languages and Systems: Companion Proceedings (MODELS ’22)*, ACM, Oct. 2022, pp. 468–472. doi:10.1145/3550356.3561589.
- [29] J. Pearl, *Causality: Models, Reasoning and Inference*, 2nd ed., Cambridge University Press, USA, 2009.
- [30] J. Pearl and D. Mackenzie, *The Book of Why: The New Science of Cause and Effect*, Basic Books, 2019. doi:10.1126/science.aau9731.
- [31] J. Peters, D. Janzing, and B. Schölkopf, *Elements of Causal Inference: Foundations and Learning Algorithms*, The MIT Press, 2017.
- [32] P. Spirtes, C. Glymour, and R. Scheines, *Causation, Prediction, and Search*, Lecture Notes in Statistics, Springer New York, 1993. doi:10.1007/978-1-4612-2748-9.
- [33] G. W. Imbens and D. B. Rubin, *Causal Inference for Statistics, Social, and Biomedical Sciences: An Introduction*, Cambridge University Press, 2015. doi:10.1017/cbo9781139025751.
- [34] M. A. Hernán and J. M. Robins, *Causal Inference: What If*, Chapman & Hall/CRC, 2024.
- [35] C. Glymour, K. Zhang, and P. Spirtes, “Review of Causal Discovery Methods Based on Graphical Models,” *Frontiers in Genetics*, vol. 10, Jun. 2019. doi:10.3389/fgene.2019.00524.

- [36] E. H. Simpson, “The Interpretation of Interaction in Contingency Tables,” *Journal of the Royal Statistical Society Series B: Statistical Methodology*, vol. 13, no. 2, pp. 238–241, Jul. 1951. doi:10.1111/j.2517-6161.1951.tb00088.x.
- [37] J. Runge, P. Nowack, M. Kretschmer, S. Flaxman, and D. Sejdinovic, “Detecting and quantifying causal associations in large nonlinear time series datasets,” *Science Advances*, vol. 5, no. 11, Nov. 2019. doi:10.1126/sciadv.aau4996.
- [38] S. W. Mogensen, K. Rathsman, and P. Nilsson, “Causal discovery in a complex industrial system: A time series benchmark,” in F. Locatello and V. Didelez, Eds., *Proceedings of Machine Learning Research*, vol. 236, ML Research Press, 2024, pp. 1218–1236. 3rd Conference on Causal Learning and Reasoning, CLear 2024, Apr. 01–03, 2024.
- [39] G. Sanf elix-Gimeno and A. Garc a-Sempere, “Book review,” *Gaceta Sanitaria*, vol. 39, p. 102487, 2025. doi:10.1016/j.gaceta.2025.102487.